Comparing vineyard imagery acquired from Sentinel-2 and Unmanned Aerial Vehicle (UAV) platform

Marco Sozzi, Ahmed Kayad, Francesco Marinello, James Taylor, Bruno Tisseyre

Received: 18 August 2019 | Accepted: 18 March 2020 | Published: 2 April 2020
DOI:10.20870/oeno-one.2020.54.2.2557

OENO One
VINE AND WINE OPEN ACCESS JOURNAL

Comparing vineyard imagery acquired from Sentinel-2 and Unmanned Aerial Vehicle (UAV) platform

Marco Sozzi[1], Ahmed Kayad[1], Francesco Marinello[1,2], James A. Taylor[3] and Bruno Tisseyre[3]

[1]University of Padova, Dept. LEAF, Viale dell'Università 16, Legnaro (PD), Italy
[2]NEOS srl, Spin-off of the University of Padova, Piazzetta Modin, 12, Padova (PD), Italy
[3]ITAP, IRSTEA, Montpellier SupAgro, University of Montpellier, Bât. 21, 2 Pl. Pierre Viala, Montpellier, France

*corresponding author: marco.sozzi@phd.unipd.it

ABSTRACT

Aim: The recent availability of Sentinel-2 satellites has led to an increasing interest in their use in viticulture. The aim of this short communication is to determine performance and limitation of a Sentinel-2 vegetation index in precision viticulture applications, in terms of correlation and variability assessment, compared to the same vegetation index derived from an unmanned aerial vehicle (UAV). Normalised difference vegetation index (NDVI) was used as reference vegetation index.

Methods and Results: UAV and Sentinel-2 vegetation indices were acquired for 30 vineyard blocks located in the south of France without inter-row grass. From the UAV imagery, the vegetation index was calculated using both a mixed pixels approach (both vine and inter-row) and from pure vine-only pixels. In addition, the vine projected area data were extracted using a support vector machine algorithm for vineyard segmentation. The vegetation index was obtained from Sentinel-2 imagery obtained at approximately the same time as the UAV imagery. The Sentinel-2 images used a mixed pixel approach as pixel size is greater than the row width. The correlation between these three layers and the Sentinel-2 derived vegetation indices were calculated, considering spatial autocorrelation correction for the significance test. The Gini coefficient was used to estimate variability detected by each sensor at the within-field scale. The effects of block border and dimension on correlations were estimated.

Conclusions: The comparison between Sentinel-2 and UAV vegetation index showed an increase in correlation when border pixels were removed. Block dimensions did not affect the significance of correlation unless blocks were < 0.5 ha. Below this threshold, the correlation was non-significant in most cases. Sentinel-2 acquired data were strongly correlated with UAV-acquired data at both the field (R^2 = 0.87) and sub-field scale (R^2 = 0.84). In terms of variability detected, Sentinel-2 proved to be able to detect the same amount of variability as the UAV mixed pixel vegetation index.

Significance and impact of the study: This study showed at which field conditions the Sentinel-2 vegetation index can be used instead of UAV-acquired images when high spatial resolution (vine-specific) management is not needed and the vineyard is characterised by no inter-row grass. This type of information may help growers to choose the most appropriate information sources to detect variability according to their vineyard characteristics.

KEYWORDS

precision viticulture, remote sensing, spatial correlation, vineyard segmentation

INTRODUCTION

Precision viticulture (PV) has been suggested as an effective approach to reach the high-quality standards required for wine production (Bramley and Hamilton, 2007). In PV, sensors are used to detect inter-field and sub-field variability in order to allow the application of site-specific management for the most important field operations (i.e. fertilising, trimming or harvesting) (Llorens *et al.*, 2010). Although high-resolution and proximal sensors may be used in PV, lower-resolution remote-sensing applications, such as satellite imagery, have proved to be challenging due to peculiarities in vineyards such as vegetation within inter-rows or diversity of training systems. However, remote sensors allow the collection of a significant amount of data in a short time, and performances are rapidly improving (Marinello *et al.*, 2019). The most common remote-sensing platforms in viticulture are unmanned aerial vehicles (UAV), airborne sensors and satellites (Hall *et al.*, 2002; Matese and Di Gennaro, 2015). UAV and airborne sensors provide high-resolution imagery (spatial, spectral and radiometric) that can be implemented in order to extract various types of vineyard information (Pichon *et al.*, 2019), however, these are expensive, limited in the area of acquisition possible, and require specialised postprocessing to achieve good final imagery (Candiago *et al.*, 2015). Conversely, satellites are more time effective and cheaper for large areas, but they are less adaptive to the growers' needs in terms of revisit time and spatial resolution (Sozzi *et al.*, 2019). High-resolution satellites (below 1 m of spatial resolution) were shown to be potentially useful in assessing leaf area of vines (Johnson *et al.*, 2003). In the last few years, the availability of free-of-charge data from satellites such as Sentinel-2 (European Space Agency) has caused increased interest in its potential use in viticulture. Sentinel 2 is a constellation of two satellites with polar orbits. Sentinel 2A was launched in 2015 and Sentinel 2B was launched in 2017. Since 2018 Sentinel 2 constellation has provided images every 5 days. Both satellites carry a multispectral imaging sensor (MSI) able to acquire images from 433 nm up to 2280 nm, in 13 bands. Red (665 nm) and near-infrared (842 nm) are of particular interest for agriculture application as they make it possible to retrieve several vegetation indices at 10 m of spatial resolution.

Recent studies have demonstrated the potential of Sentinel-2 images in viticulture at a territorial scale to extract agronomic information and to quantify the impact of drought (Devaux *et al.*, 2019; Cogato *et al.*, 2019).

In this study, performances and limitations of Sentinel-2 imagery in vineyards without inter-row grass were assessed, based on the normalised difference vegetation index (NDVI) (Rouse *et al.*, 1973). The ability of satellite NDVI images to characterise variability at field and sub-field scale were estimated using the Gini coefficient (Gini, 1921). To achieve these objectives, Sentinel-2 NDVI was compared to UAV extracted data as a reference layer.

MATERIALS AND METHODS

1. Study area

For the study, 30 non-irrigated vineyard blocks in the Minervois *Appellation d'Origine Contrôlée* in the Languedoc-Roussillon region in the south of

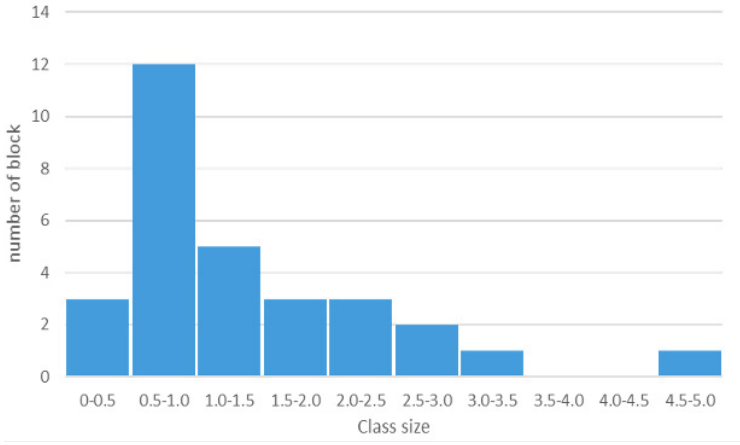

FIGURE 1. Block size distribution: in the selected study area, 20 blocks were less than 1.5 hectares and 10 blocks were between 1.5 and 5 hectares.

France (43°18'25'' N, 2°37'21'' E, WGS84) were selected. The selected blocks were trained using vertical shoot positioning (VSP), with an inter-row space ranging from 2.0 to 2.5 m without any vegetation cover. The planting dates ranged from 2003 to 2011. The mean block area was 1.4 ha, with a minimum and maximum area of 0.22 and 4.9 ha, respectively (Figure 1). The features of the correspond to the ordinary vineyard conditions in the Languedoc-Roussillon region.

2. Data acquisition and processing

The NDVI (Rouse *et al.*, 1973) was selected because it is one of the most common vegetative indices used in agriculture (Psomiadis *et al.*, 2017). Data acquisition was performed on August 2016. Blocks borders were delineated using high-resolution images in Google Earth Pro (Google Inc., Mountain View, CA, USA). The UAV images were acquired on 22 August 2016 by means of a multispectral camera MicaSense RedEdge-MX. UAV-acquired data were converted to reflectance based on the measurement in the field of a calibrated reflectance target. All collected images were elaborated through a standard photogrammetry process, then orthorectified and tiled. Orthorectification, mosaicing and resampling were performed using Pix4D software (Pix4D S.A., Prilly, Switzerland) by the UAV operator (DELAIR, Toulouse, France). As a result of this process, a multispectral image, with a spatial resolution of 0.08 m, was obtained for all blocks.

The Sentinel-2 imagery was downloaded from the official Copernicus Open Access Hub (www.scihub.copernicus.eu). A 1C product acquired on 26 August 2016 was selected and downloaded due to the lack of 2A products (not provided before May 2017). The atmospheric correction was carried out using SNAP software (ESA, European Union).

From the UAV and Sentinel-2 imagery there were four defined datasets (layers): three were extracted from the UAV imagery and one from Sentinel-2 imagery. The Sentinel-2 imagery (10 m pixel) was chosen as reference spatial resolution for the upscaling of other layers. The UAV extracted layers were considered as a reference of vineyard conditions at field level.

For the first layer extracted from UAV, the images were clipped to the polygon of each block and then NDVI was calculated for all pixels within the block using the formula proposed by Rouse *et al.* (1973). This layer was then upscaled to the Sentinel-2 spatial resolution using the mean value of the pixel located in the same area (10 m). Such upscaling methodology is commonly implemented for this type of analysis (Matese *et al.*, 2015; Qin *et al.*, 2015). The result of this upscaling process corresponds to UAV NDVI mixed 10 m (point 1 in Figure 2).

The second layer consisted of the selection of vine-only pixels in UAV imagery, achieved by removing inter-row and potentially mixed pixels. This process was carried out using a supervised classification process. Taking advantage of the classification wizard in ArcGIS Pro 2.4 (ESRI, Redlands, CA, USA), a multiclass support vector machine (SVM) algorithm was trained using 850 polygons

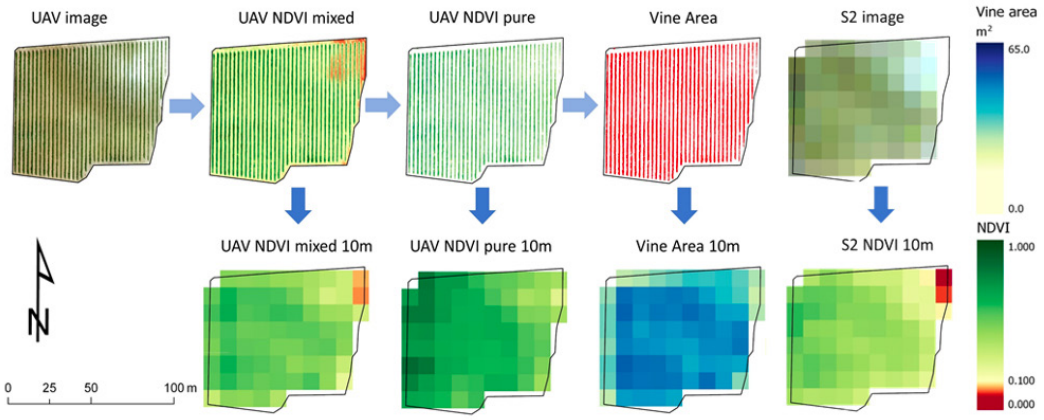

FIGURE 2. Processing flow applied to datasets.
NDVI was extracted from UAV multispectral image (UAV NDVI mixed), then was segmented to obtain pure vine index (UAV NDVI pure) and vine area. These three datasets were upscaled to the same resolution on Sentinel-2 image (10×10 m). NDVI Sentinel-2 were calculated from multispectral Sentinel-2 image

manually classified into four classes: high vigour vine, low vigour vine, soil, and shadow. This learning dataset covered an area of 718 m^2 (0.1 % of the total area). The segmentation algorithm was trained considering spectral and shape features of grouped UAV NDVI mixed pixels. The accuracy assessment of the classification process was performed using Cohen's kappa, which is based on a confusion matrix of true positive/negative and false positive/negative. The final Cohen's kappa of the SVM classification algorithm was 0.86. Pixels arising from high vigour and low vigour vines were merged and extracted as a shapefile. This pure vine mask was used to clip the original UAV NDVI image. The resulting raster was filled with zero NDVI value in the inter-row (non-vine) space, in order to simulate a no effect of soil in terms of NDVI. Then, the raster was upscaled using the same methodology described for the UAV NDVI mixed layer. The result of this workflow corresponds to UAV NDVI pure 10 m pixels (point 2 in Figure 2) and it only considers the vine response.

The pure vine mask was also used to extract the projected vine area per pixel. This latter parameter is abbreviated in the following paragraphs as Vine Area, although it represents the planar vine area and not the vine area commonly defined in viticulture (total area of the canopy). The pixel grid of the Sentinel-2 product was intersected with the pure vine mask to obtain the value in square metres of vine over a 10 m pixel. This layer corresponds to vine area 10 m (point 3 in Figure 2).

The Sentinel-2 NDVI (S2 NDVI) was calculated with band 4 (Red) and band 8 (near-infrared), obtaining an NDVI image with 10 m pixel resolution. The last step of satellite image processing was to clip the NDVI according to the border of each block, done by means of ArcGIS Pro 2.4 software. The result of these processes corresponds to S2 NDVI 10 m (point 4 in Figure 2).

Partially different spectral and optical properties characterise the Sentinel-2 and MicaSense-MX sensors. However, when accounting for the major sensitivity of silicon sensors to the central wavelength, differences in bandwidths were considered to be negligible in the calculation of NDVI and for other reported analyses.

3. Statistical analysis

Data were analysed using four different approaches. First, the border effect on S2 NDVI was evaluated in comparison to UAV NDVI pure. Even if some studies have already applied masks for border effects, a statistical justification is still missing (Devaux *et al.*, 2019). In the second and third approaches, each block was analysed singularly (sub-field scale) and in relation to all other blocks (inter-field scale). Pearson's correlation coefficient was used to compare the similarity between different information sources. The Dutilleul correction was applied to account for spatial autocorrelation of data (Dutilleul *et al.*, 1993) in sub-field scale analysis. Spatial autocorrelation may violate the assumption of independence in the correlation analysis, leading to a biased estimation of variances and correlation coefficient (Dutilleul *et al.*, 1993). Although the Dutilleul correction is commonly applied in ecology, it is not widespread in agricultural studies, which often overestimate the significance of the Pearson's coefficient in spatial datasets (Taylor and Bates, 2013). The analysis at sub-field level was performed using PASSaGE v2 software (Pattern Analysis, Spatial Statistics and Geographic Exegesis; Tempe, AR, USA) to calculate the modified significance test as proposed by Dutilleul (Rosenberg and Anderson, 2011). The field-scale comparison was performed without considering spatial autocorrelation, as each block can be considered an independent observation. In order to compare data acquired from different sensors, correlations between all four layers (S2 NDVI, UAV NDVI mixed, UAV NDVI pure, and Vine Area) were also analysed, considering effects of borders and block dimensions.

Additionally, the variability of each layer was estimated using the Gini coefficient (Gini, 1921) to highlight the magnitude of variation of each block in each layer. The use of the Gini coefficient in agriculture is not common, even though it is useful in describing the inequality in a distribution (Sadras and Bongiovanni, 2004; Woodward *et al.*, 2007). To calculate G, all observations (S2 NDVI, UAV NDVI mixed, UAV NDVI pure, and Vine Area) were ranked for each block from smallest to largest, then the cumulative fraction of each variable was plotted against the cumulative fraction of the population. In case of perfect equality (low variability) the cumulative fraction of the variable corresponds to the cumulative fraction of population. The Gini coefficient (G) was calculated according to the following formula:

$$G = \frac{\sum Population\ fraction - \sum Variable\ fraction}{\sum Variable\ fraction}$$

RESULTS

1. Border effect and block dimension evaluation

The first analysis compared the sub-field correlation between S2 NDVI and UAV NDVI pure, with this latter layer considered as a reference for the block variability. The correlations were calculated using 10×10 m pixel information and considering the whole block and the block after removing border pixels (within 10 m of the block boundary) on the S2 NDVI. This test was carried out to evaluate the influence of border pixels, which might be mixed (vineyard and headland).

The *r* values computed with the whole blocks (including border pixels) had a wide range of variation, with 93 % of *r* values (28/30 blocks) ranging from 0.52 up to 0.93, and two extreme values of -0.32 and 0.45. When the border pixels were removed, 93 % of *r* values (28/30 blocks) ranged from 0.76 to 0.97 with two extreme values of 0.07 and 0.56. The border pixel removing process influenced the correlation coefficient, leading to an increase of the mean *r* (from 0.772 to 0.837) but conversely decreased (from 29 to 27) the number of blocks with a significant correlation (Table 1).

TABLE 1. Distribution of correlation coefficients and their significance between S2 NDVI and the upscaled (10×10 m) UAV NDVI derived from pure vine pixels only when the border pixels are kept (Whole) and when these pixels are removed (Border removed). Significance was assessed with Dutilleul correction for spatial autocorrelation.

	Whole	Border removed
Mean	0.772	0.837
Dev.St	0.147	0.164
Count (n. field)	30	30
Significant at $p < 0.05$	29	27
Not significant	1	3
Only significant fields p < 0.05		
Mean (only significant)	0.787	0.865
Dev.st (only significant)	0.123	0.083

Figure 3 shows how the significance of the correlation between S2 NDVI (without border pixels) and NDVI pure was affected by block area. According to Figure 3, non-significant correlations occurred in smaller blocks (0.193 ha), whereas the average area of the blocks where it was significant was larger (1.03 ha).

The difference between the average block area of both groups was significant (t-test, $p < 0.001$).

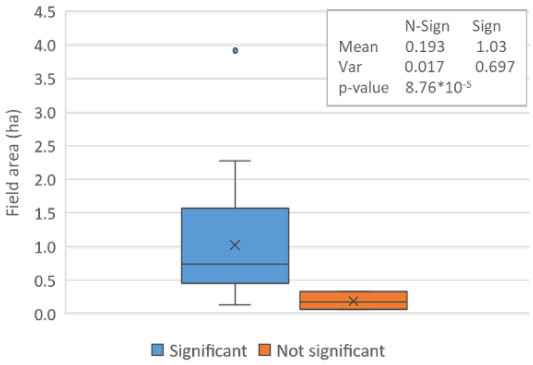

FIGURE 3. Effect of block area on the significance of correlation (with the Dutilleul correction) between S2 NDVI (after border pixel removal) and the UAV NDVI derived from pure vine-only pixels. The embedded table indicates the mean and variance associated with the two groupings.

2. Sub-field scale correlation

In agreement with results reported in the previous paragraph, the following analysis focuses only on data (layers) where border pixels have been removed.

The sub-field correlation coefficients were calculated between S2 NDVI and the other three datasets (UAV NDVI mixed, UAV NDVI pure, and Vine Area), again adjusting the significance test using the Dutilleul correction. The comparison of the Pearson's coefficient distribution is reported in Table 2. At the sub-field scale, the average correlation between S2 NDVI and UAV NDVI pure was 0.837, for UAV NDVI mixed it was 0.834, and for Vine Area it was 0.798. A different ranking was found for the standard deviation of Pearson's coefficient, which decreased from UAV NDVI pure to UAV NDVI mixed.

Table 2 also reports the average correlation coefficients between S2 NDVI and all the other three datasets when blocks with only significant correlation were considered. In this case, an overall increase of correlation and decrease of standard deviation was found. Moreover, the highest correlation was reached by the couple S2 NDVI – UAV NDVI mixed, which is characterised by the same mixed pixel composition.

3. Field-scale correlation

The following analysis was carried out considering mean block values, rather than the pixel-wise

TABLE 2. Descriptive statistics of correlation for all block considered calculated using Dutilleul correction for significance test.

	S2 Vs UAV NDVI Pure	S2 Vs UAV NDVI Mixed	S2 vs Vine Area
Pearson (mean)	0.837	0.834	0.798
Pearson (dev.st)	0.164	0.215	0.210
Count (n. fields)	30	30	30
Significant at $p < 0.05$	27	27	28
Not significant	3	3	2
Only significant fields p < 0.05			
Pearson (mean, only significant)	0.865	0.875	0.831
Pearson (dev.st, only significant)	0.083	0.079	0.096

At sub-field scale, S2 NDVI is more correlated with UAV NDVI mixed than Vine Area than UAV NDVI pure.

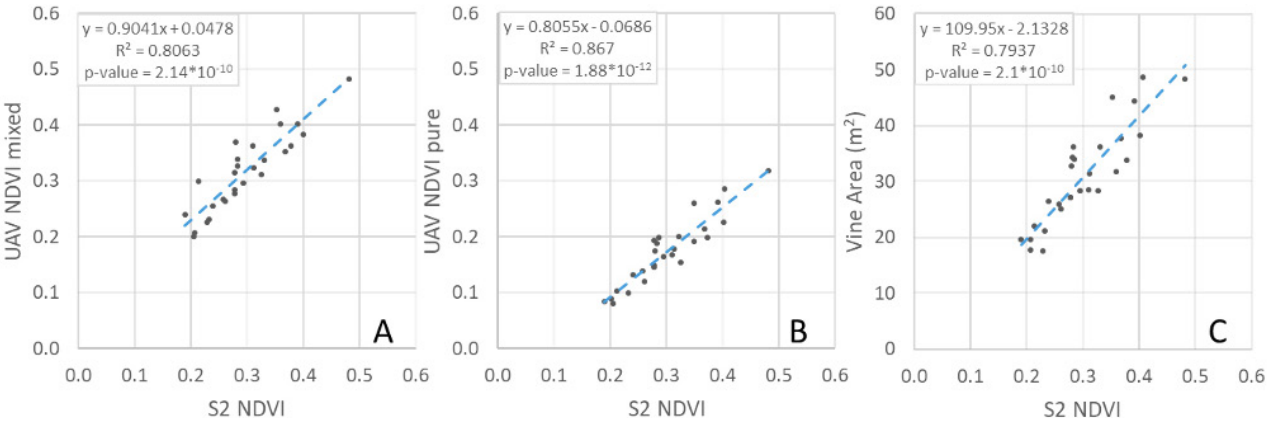

FIGURE 4. Regression models between S2 NDVI and UAV-derived datasets based on the mean value of blocks.

comparisons implemented in the case of Results 1 and 2. The analysis were focused on blocks where significant correlation ($p < 0.05$) at sub-field scale was found. In this case, measurements were considered to be independent (with no spatial autocorrelation), and the significance test was done without the Dutilleul correction.

Figure 4 shows three linear regression models fitting the three UAV-derived layers to the S2 NDVI layer. The R^2 values of the linear regressions between S2 NDVI and UAV NDVI mixed, UAV NDVI pure and Vine Area were 0.81, 0.87, and 0.79, respectively. R^2 was significant in all cases ($p < 0.01$), which is evidence of a relevant link between S2 NDVI and all derived UAV indices. Considering slope and intercepts, UAV NDVI mixed and Vine Area are proportionally correlated with S2 NDVI (1:1 regression), while UAV NDVI pure exhibits lower variance than S2 NDVI.

4. Gini coefficient interpretation

Figure 5 shows the boxplot graph of Gini coefficient (G) distribution, which explains the variability of the four layers. A similar G distribution was found between S2 NDVI and UAV NDVI mixed. Such behaviour was caused by the similar mixed pixel composition of the two layers. In the same way, a similar distribution was found between UAV NDVI pure and Vine Area. In this case, the similarity was a result of the two layers only including information related to the vine response (and masking the inter-row response).

Figure 5 reports also some example values of NDVI and G, with respective maps. In the case of Field 1, a low value of NDVI was combined with a high G while, in Field 2, a high NDVI was paired with a low G. These examples suggest that in case of high average NDVI, this might be not equally distributed over the block.

DISCUSSION

The comparison between NDVI from Sentinel-2 and pure vine NDVI extracted from UAV images showed an increasing correlation if the border pixels were removed from the satellite's images. According to this result, it is advisable to remove

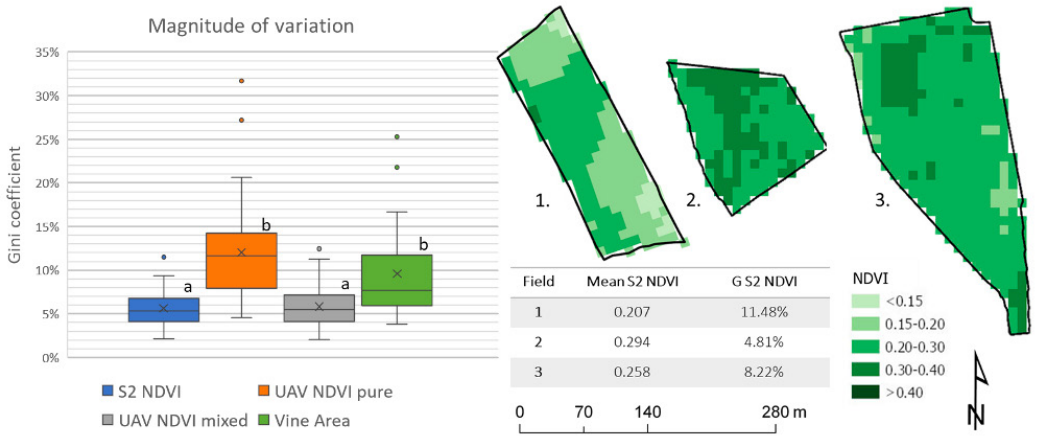

FIGURE 5. Range of variation, expressed using the Gini coefficient in boxplot form, in the four layers across 30 vineyard blocks. Three example blocks are shown to visually illustrate the variability in the S2 NDVI response across blocks. For each block the field-specific mean S2 NDVI and G value are also provided.

border pixels of Sentinel-2 imagery for viticulture applications. Edge effects are introducing uncertainty into the spectral response and the information at the borders is less indicative of actual vine properties. However, the process for removing border pixels is problematic in smaller blocks, because such borders constitute a large percentage of the whole block pixels. For blocks < 0.5 ha, removal of border pixels can lead to a decrease in the significance of correlation between satellite and UAV layers. According to these considerations, Sentinel-2 images with border pixels removed can be used for blocks larger than 0.5 ha, whereas for smaller blocks (<0.5 ha), the satellite imagery is less reliable. For these blocks higher resolution sensing is required, such as UAV-acquired images. This characteristic is an important limitation for the use of Sentinel-2 images for viticulture regions with small vineyard blocks.

When Sentinel-2 images are acquired in larger blocks (>0.5 ha), they can be used to compare different vineyard blocks, considering the mean block values (inter-field comparison). In this situation, Sentinel-2 images can therefore constitute a relevant decision support for advisory services to manage vigour or vegetative expression or for any other application requiring the characterisation of the vegetative expression levels of blocks at a denomination or regional scale. However, end-users still need to be conscious that the Sentinel-2 mixed pixels integrate information about the spectral properties of vines, the projected vine area, and inter-row space and training systems, which may affect comparisons and decisions.

However, for blocks larger than 0.5 ha, Sentinel-2 images may well be used to characterise the within-field variability. Indeed, this study shows that they can constitute an interesting decision-making support for the following: i) identifying blocks with high spatially organised variability (Leroux and Tisseyre, 2019); ii) prioritising blocks on which spatial variability requires the use of differentiated management strategies at the within-field level; and iii) possibly defining within-field management zones or broad trends in vine properties. This is in contrast with other reported studies of satellite imagery in viticulture (Khaliq *et al.*, 2019). However, it is necessary to consider that the 10 m mixed pixels do smooth the real magnitude of variation of vine properties (with UAV NDVI of pure vines as a reference) and cannot be used for any vine-specific application. It is recommended that variability revealed by Sentinel-2 and other medium-resolution sensors should not be compared without considering this latter point. The results of this study in terms of R^2 between S2 NDVI and UAV NDVI mixed are comparable to other studies. Conversely, the R^2 between S2 NDVI and UAV NDVI pure is higher than seen in previous work (Di Gennaro *et al.*, 2019). This latter condition may be ascribable by the simulation of no soil effects on NDVI performed in this study.

All the analyses performed in this study were applied to blocks without cover crops in the inter-row space. The presence of an inter-row crop would introduce additional noise to spectral data, and misleading considerations could be drawn. This study cannot be used to validate the use of

Sentinel-2 imagery (or any medium-resolution sensor with mixed pixels) in vineyard blocks with inter-row growth. Indeed, the spectral information on inter-row crops cannot be divided by the vine signal, leading to an erroneous variability estimation: in this case, high-resolution images should be preferred as they allow extraction of vine pixels (Khaliq *et al.*, 2019). However it should be noticed that, at present, the majority of vineyards are not irrigated; due to the summer water deficit, the inter-row grass is dry at the beginning of the summer, thus at an NDVI state that does not differ too much from the zero NDVI condition simulated for the present work. Therefore, at veraison, the effect of inter-row grass may be considered negligible (Kazmierski *et al.*, 2011).

CONCLUSION

Vegetation index patterns in vineyard blocks with no inter-row cropping were similar for Sentinel-2 imagery (medium resolution) and high-resolution UAV imagery upscaled to a medium-resolution. There were effects on the canopy vigour pattern associated with pixels along the border of blocks, which is likely due to variable mixed pixel effects at the vineyard border. Removing border pixels is recommended when analysing Sentinel-2 imagery of vineyards, but this is only feasible in blocks >0.5 ha. For blocks <0.5 ha, Sentinel-2 imagery applications appear limited. For broad canopy and vine management decisions within and between vineyard blocks, Sentinel-2 imagery appears just as useful as high-resolution UAV/aerial imagery and should provide cost and access benefits (Sozzi *et al.*, 2019). Sentinel-2 imagery cannot currently provide vine-specific information and high-resolution imagery is required for such applications. These results are not transferable to vineyard blocks with inter-row growth; indeed, the experimentation was carried out in blocks without inter-row grass coverage.

Acknowledgements: The present work was founded by Fondazione Ing. Aldo Gini (Padova, Italy). The authors would like to acknowledge TerraNIS SAS (Ramonville-St-Agne, Occitanie, France) and Sylvie Duthoit for UAV images supply. UAV data acquisition campaign was partly funded within the regional OENOMIP project which was co-funded by the European Union.

REFERENCES

Bramley R.G.V. and Hamilton R.P., 2007. Terroir and precision viticulture: Are they compatible? *Journal International Des Sciences de La Vigne et Du Vin*, *41*(1), 1–8. doi:10.20870/oeno-one.2007.41.1.855

Candiago S., Remondino F., De Giglio M., Dubbini M. and Gattelli M., 2015. Evaluating multispectral images and vegetation indices for precision farming applications from UAV images. *Remote sensing*, 7(4), 4026–4047. doi:10.3390/rs70404026

Cogato A., Pagay V., Marinello F., Meggio F., Grace P. and De Antoni Migliorati M., 2019. Assessing the Feasibility of Using Sentinel-2 Imagery to Quantify the Impact of Heatwaves on Irrigated Vineyards. *Remote Sensing*, 11(23), 2869. doi:10.3390/rs11232869

Devaux N., Crestey T., Leroux C. and Tisseyre B., 2019. Potential of Sentinel-2 satellite images to monitor vine fields grown at a territorial scale. *OENO One*, *53*(1). doi:10.20870/oeno-one.2019.53.1.2293

Di Gennaro S.F., Dainelli R., Palliotti A., Toscano P. and Matese A., 2019. Sentinel-2 Validation for Spatial Variability Assessment in Overhead Trellis System Viticulture Versus UAV and Agronomic Data. *Remote Sensing,* 11(21), 2573. doi:10.3390/rs11212573

Dutilleul P., Clifford P., Richardson S. and Hemon D., 1993. Modifying the t Test for Assessing the Correlation Between Two Spatial Processes. *Biometrics*, *49*(1), 305–314. doi:10.2307/2532625

Gini C., 1921. Measurement of Inequality of Incomes. *The Economic Journal*, *31*(121), 124. doi:10.2307/2223319

Hall A., Lamb D.W., Holzapfel B. and Louis J., 2002. Optical remote sensing applications in viticulture - a review. *Australian Journal of Grape and Wine Research*, *8*(1), 36–47. doi:10.1111/j.1755-0238.2002.tb00209.x

Johnson L.F., Roczen D.E., Youkhana S.K., Nemani R.R. and Bosch D.F., 2003. Mapping vineyard leaf area with multispectral satellite imagery. *Computers and electronics in agriculture*, 38(1), 33-44. doi:10.1016/S0168-1699(02)00106-0

Khaliq A., Comba L., Biglia A., Ricauda Aimonino D., Chiaberge M. and Gay P., 2019. Comparison of Satellite and UAV-Based Multispectral Imagery for Vineyard Variability Assessment. *Remote Sensing*, 11(4), 436.

Leroux C. and Tisseyre B., 2019. How to measure and report within-field variability: a review of common indicators and their sensitivity. *Precision Agriculture*, *20*(3), 562–590. doi:10.1007/s11119-018-9598-x

Llorens J., Gil E., Llop J. and Escolà A., 2010. Variable rate dosing in precision viticulture: Use of electronic devices to improve application efficiency. *Crop Protection*, *29*(3), 239–248. doi:10.1016/j.cropro.2009.12.022

Marinello F., Bramley R.G.V., Cohen Y., Fountas S., Guo H., Karkee M., Martìnez-Casanovas J.A, Paraforos D.S, Sartori L., Sorensen C.G, Stenberg B., Sudduth K., Tisseyre B, Vellidis F. and Vougioukas S.G., 2019. Agriculture and digital sustainability: a Digitization Footprint. In *Precision agriculture '19* (pp. 83–89). The Netherlands: Wageningen Academic Publishers. doi:10.3920/978-90-8686-888-9_9.

Matese A. and Di Gennaro S.F., 2015. Technology in precision viticulture: a state of the art review. *International Journal of Wine Research*, *7*, 69. doi:10.2147/IJWR.S69405

Matese A., Toscano P., Di Gennaro S.F., Genesio L., Vaccari F.P., Primicerio J., Belli C., Zaldei A., Bianconi R. and Gioli B., 2015. Intercomparison of UAV, aircraft and satellite remote sensing platforms for precision viticulture. *Remote Sensing*, *7*(3), 2971–2990. doi:10.3390/rs70302971

Pichon L., Leroux C., Macombe C., Taylor J. and Tisseyre B., 2019. What relevant information can be identified by experts on unmanned aerial vehicles' visible images for precision viticulture? *Precision Agriculture*, 1–17. doi:10.1007/s11119-019-09634-0

Psomiadis E., Dercas N., Dalezios N.R. and Spiropoulos N.V., 2017. Evaluation and cross-comparison of vegetation indices for crop monitoring from sentinel-2 and worldview-2 images. In C.M. Neale & A. Maltese (Eds.), *Remote Sensing for Agriculture, Ecosystems, and Hydrology XIX* (Vol. 10421, p. 79). SPIE. doi:10.1117/12.2278217

Qin J., Zhao L., Chen Y., Yang K., Yang Y., Chen Z. and Lu H., 2015. Inter-comparison of spatial upscaling methods for evaluation of satellite-based soil moisture. *Journal of Hydrology*, *523*, 170–178. doi:10.1016/J.JHYDROL.2015.01.061

Rosenberg M.S. and Anderson C.D., 2011. PASSaGE: Pattern Analysis, Spatial Statistics and Geographic Exegesis. Version 2. *Methods in Ecology and Evolution*, *2*(3), 229–232. doi:10.1111/j.2041-210X.2010.00081.x

Rouse J.W., Hass R.H., Schell J.A., Deering, D.W., 1973. Monitoring vegetation systems in the great plains with ERTS. *Third Earth Resources Technology Satellite (ERTS) Symposium*, *1*(1), 309–317. doi:citeulike-article-id:12009708

Sadras V. and Bongiovanni R., 2004. Use of Lorenz curves and Gini coefficients to assess yield inequality within paddocks. *Field Crops Research*, *90*(2–3), 303–310. doi:10.1016/J.FCR.2004.04.003

Sozzi M., Kayad A., Giora D., Sartori L. and Marinello F., 2019. Cost-effectiveness and performance of optical satellites constellation for Precision Agriculture. In *Precision agriculture '19* (pp. 501–507). The Netherlands: Wageningen Academic Publishers. doi:10.3920/978-90-8686-888-9_62

Taylor J.A. and Bates T.R., 2013. A discussion on the significance associated with Pearson's correlation in precision agriculture studies. *Precision Agriculture*, *14*(5), 558–564. doi:10.1007/s11119-013-9314-9

Woodward T.J., Green T.G.A. and Clearwater M.J., 2007. Between-vine variation in 'Hayward' kiwifruit vine income: The use of Lorenz curves and gini coefficients to describe variation and assess the potential for zonal management. *European Journal of Horticultural Science*, *72*(6), 280–287.